http://ansinet.com/itj

ITJ

ISSN 1812-5638

INFORMATION TECHNOLOGY JOURNAL

ANSInet
Asian Network for Scientific Information
308 Lasani Town, Sargodha Road, Faisalabad - Pakistan

Information Technology Journal 8 (5): 717-725, 2009
ISSN 1812-5638

Simulated Distribution of the Retinal Photoreceptors for Space Variant Resolution Imaging

[1]Zuojin Li, [1]Weiren Shi and [2]Zhi Zhong
[1]College of Automation, Chongqing University, Chongqing, China
[2]The Smartech Institute, Shenzhen, Guangdong, China

Abstract: This study presents a new computable method to simulate distribution of the retinal photoreceptors for space variant resolution imaging. In this presented method, first, a model of Laplacian and Gaussian multi-resolution pyramids is built; second, a weighting function coming from human visual psychological experiments is adopted in the presented model, lastly, a typical linear interpolation method is used between steps of multi-resolution pyramids. Another contribution of this study displays some experiments revealing the preliminary relationship between the place of gaze (foveation), image resolution and image compression rate. Compared with traditional uniform image processing methods, some experiment results show that the presented method in this study, approaches closer to the biological fact of visual perception and resolves the ring artifacts distortion, a problem left behind from the earlier study. The most obvious application of space variant resolution technique can be presented for digital image compression in low-bandwidth image communication.

Key words: Retinal photoreceptor, space variant resolution, multi-resolution pyramid, image compression

INTRODUCTION

The Human Visual System (HVS) is highly space-variant in sampling, coding, processing and understanding the physical world, because there are non-uniformly distributed photoreceptors at the retina. A high-concentration cone photoreceptor is located at the point of gaze. Departing from the point of gaze or central fovea, cone photoreceptors decrease significantly, while rod photoreceptors increase markedly (Wandell, 1995; Cormack, 2000). Biological research indicates that cone photoreceptors play important roles in visual perception. That is to say, where are more cone photoreceptors, there is more frequency information of the objects and the clearer the image on the retina vise versa. Further study reveals that the spatial resolution of human vision is cut in half at about 2.3° from the point of fixation at 20°, by a factor of ten. Figure 1 shows the distribution and density variation of the photoreceptors as a function of eccentricity from the retinal center.

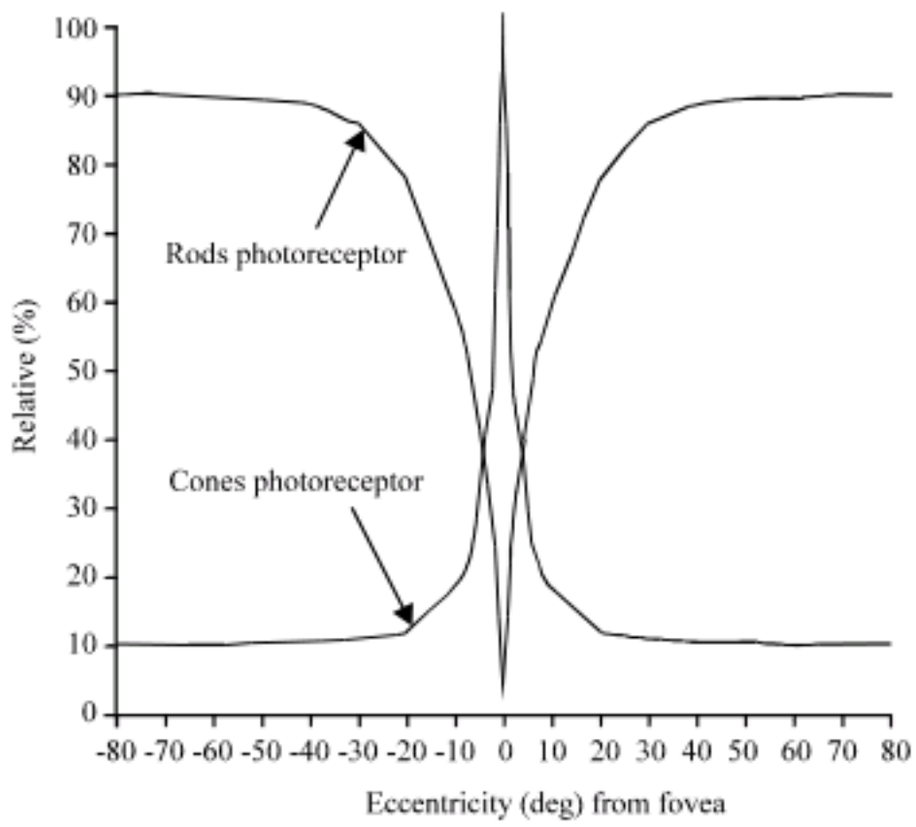

Fig. 1: The percentage distribution of rods and cones photoreceptor with retinal eccentricity

When a human observer gazes at a point in a real-word image, a variable resolution image, as a biological result, is transmitted through the front visual channel into the high level processing units in the human brain. By taking advantage of this fact, this non-uniform resolution processing can be applied to digital imaging or video transmission. This application would be valuable when the bandwidth is at a premium nowadays. For instance, consider an image database at a remote server. If the network connection between the user and the image server is slow, image compression algorithms can be vital. By contrast, traditional digital vision systems represent images on rectangular uniformly sampled lattices, which have the advantages of simple acquisition, storage,

Corresponding Author: Zuojin Li, College of Automation, Chongqing University, Chongqing, China

indexing and computation. However, in the process of simulated HVS perception, high-fidelity vision would be maintained around the point of gaze, while departing from it, varied resolution information is transmitted according to the fact of HVS perception. The high-quality image compression is thus required.

From the information processing point of view, image processing simulating biological retinal model is more efficient than traditional methods (Wang *et al*., 2007). The motivation behind foveation image processing is that there exists considerable high-frequency information redundancy in the peripheral regions, thus a much more efficient representation of images can be obtained by removing or reducing such redundancy for implementing low bandwidth communication with HVS. In this study, a computable method using Laplacian and Gaussian multi-resolution pyramids is presented to perform the simulated distribution of human retinal photoreceptors for space variant resolution imaging. The Gaussian pyramid is chosen because the non-uniformly blurred version of the uniform original image can be required based on its highly non-uniform image decomposition. The Laplacian pyramid can also improve the quality of image compression. Another crucial advantage of Laplacian and Gaussian pyramids, they allow for an arbitrary spatial resolution weighting function and thus ensure smoothness between image decomposition layers.

RELATED SPACE VARIANT RESOLUTION IMAGE PROCESSING

Four major image processing techniques inspired from the HVS have been exploited perfectly in the development of image processing system (Cormack, 2000). First, the temporal contrast sensitivity of the HVS declines at high frequencies creating a temporal resolution cutoff of approximately 60 Hz. Second, the spatial contrast sensitivity of the HVS declines at high frequencies creating a spatial resolution cutoff of approximately 50 cycles per degree. Third, chromatic information is encoded in HVS by only three broad-band photoreceptors, with peak sensitivities at 440, 540 and 570 nm. Fourth, the chromatic spatial resolution of the HVS is lower than the luminance spatial resolution by a factor of approximately two. The fifth image processing technique inspired from the HVS will be foveated imaging. Namely, the fact that the spatial resolution of HVS declines dramatically and smoothly away from the point of fixed gaze will be a useful image compression tool. In last twenty years, there has been growing recent interest in research work on foveated image processing. When rendered on screen, foveated images take up as many pixels as unfoveated images. Therefore, to realize any data savings from foveation, some algorithm must be used to generate the full image from a reduced data set. In this study, there appear to be four broad implementation approaches; geometric method, quality-based method, multi resolution method and integral operator based on kernel function.

Geometric approach that has been used to implement space-variant resolution from the uniform pre-images using the foveated retinal sampling geometry. A typically used solution is the logmap transform defined as:

$$W = \log(z + a) \tag{1}$$

where, a is a constant and z and W are complex numbers representing the positions in the original coordinate and the transformed coordinate, respectively (Wallace *et al*., 1994).

The difficulty with this method is that the image pixels originally located at integer grids are moved to non-integer positions, making them difficult to be indexed. Another geometric approach is based on super-pixel thoughts (Kortum and Geisler, 1996; Bandera and Scott, 1989; Camacho *et al*., 1996; Tsumura *et al*., 1996). There are three direct drawbacks of the super-pixel methods. First, the discontinuity across super-pixels is often very perceptually annoying. Blending methods are usually used to reduce the boundary effect, leading to additional computational cost. Second, most of these methods result in compressed images with oddly-shaped boundaries, which are often difficult to transmit and decode in a standard way. In addition, many of the resolution functions used have singularities at the fovea, meaning that special processing must be used in the area of highest fidelity. Finally, these algorithms become even more difficult to implement if the fovea does not lie at the image center. Because of their inflexibility, these algorithms are seldom used for general-purpose image foveation.

Quality-based foveated imaging approach is found in the study (Tsumura *et al*., 1996; Lee *et al*., 2001, 2002), which are closer to the HVS than the geometric approach presented in the paragraph above. As a type example, variable-quality DCT compression is described by Tsumura *et al*. (1996) in standard block DCT compression, a single quality factor is set for the entire image and the image is uniformly degraded by that factor. To foveate such an image, the quality factor is allowed to vary for each 8×8 DCT block. At blocks close to the fovea center, the quality factor approaches 100%. As blocks get further from the fovea, the quality factor decreases in proportion to visual acuity. Since, lower quality factors

generally mean that higher spatial frequencies will be represented more poorly, the net effect is to reduce spatial resolution away from the fovea. The maximum degradation is constrained by the size of DCT blocks. While, this approach shows promise, it is unclear how the spatial sensitivity of the human visual system can be correlated with DCT quality factors. Block boundary artifacts also become a problem at locations far from the fovea.

Taking the advantage of multi-resolution, Geisler and Perry (1998) and Kuyel *et al*. (1999) have proposed the use of an image pyramid representation for foveated imaging. In a standard image pyramid, as described by Geisler and Perry (1998), the image is blurred and subsampled repeatedly to create a number of copies of the original image with different resolutions. In a foveated approach, the image pyramid represents less and less of the image as it reaches the top. This manner of image decompression lends itself to fovea-first transmission. If the foveal regions of the pyramid are transmitted first, then the remaining data can easily be transmitted later without any redundant data transmission. A very slight penalty will be paid over the unfoveated pyramid transmission in order to transmit the coordinates of each foveation subregion. There has been a proliferation of literature in recent years with various wavelet transforms for multi-resolution foveated imaging (Chang and Yap, 1997; Chang *et al*., 2000; Wang and Bovik, 2000).

Finally, there has been some study in recent years attempting to use pure math operator with different parameter models and kernel function for foveated images and reconstruction of their uniform pre-images (Somma, 2006; Didenko *et al*., 2007; Itti, 2004; Thamcheewan *et al*., 2007; Kumwilaisak, 2008; Chang *et al*., 2008). First, different models will be applied in foveation based on image content. Some results based on models have more difference with the fact of HVS in space-variant resolution, while have more simple computation in image transmission system. Second, approximate foveated images can be obtained from uniform images via., the approximation of some integral operators. It is shown that these operators belong to a well-studied operator algebra and the problem of restoration of the approximate uniform pre-images is feasible. But, selecting kernel function will be difficult because of variant necessary and sufficient conditions of integral operators based on different kernel function.

SPACE VARIANT RESOLUTION IMAGING BASED ON MULTI-RESOLUTION PYRAMID AND ITS IMAGE COMPRESSION

In order to generate space variant imaging simulating foveated images, an original uniform-resolution image is

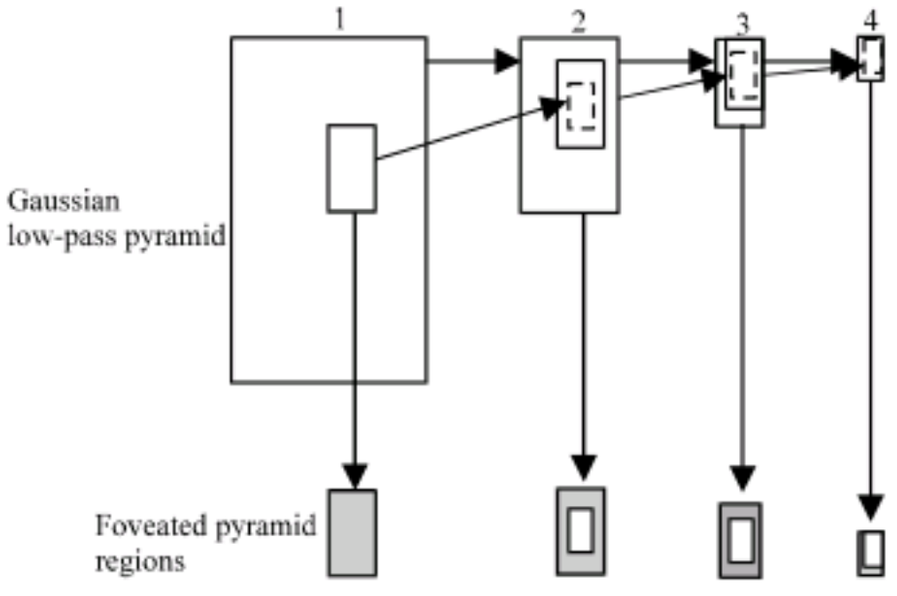

Fig. 2: Multi-resolution pyramid based on Gaussian low-pass filter and foveated procession

decomposed into a Gaussian pyramid of several levels. The processing of Gaussian pyramid is generally shown in Fig. 2. The levels of this pyramid are numbered, where level 1 represents the full-sized image and each smaller-sized image occupies a higher-numbered level. That also means a region of smaller spatial extent is taken from each higher-resolution level of the pyramid. The Gaussian filter is chosen in each pyrlevel because blurred versions of the original image will be required for certain portions of the foveation process. Further, the Gaussian filter used in image preprocessing can resolve the ringing effect. Another advantage of being somewhat intuitive, they allow for an arbitrary spatial resolution weighting function and implement foveation of discretely-sampled images with smoothly varying resolution. A typical Gaussian function is shown as:

$$H(x, y) = \exp\left[-\frac{l^2(x,y)}{2\sigma_0^2}\right] \quad (2)$$

where, σ_0 is the cut-off frequency in filtering image. In this case, σ_0 is decided by weighting function presented in the following. $l(x, y)$ denotes the distance between a given point and the center in processing image.

Next, a weighing function coming from psychological experiments is adopted. A model that fits the experiment data was given by Geisler and Perry (1998):

$$CT(f, e) = CT_0 \exp\left(\alpha . f . \frac{e + e_2}{e_2}\right) \quad (3)$$

where, f is spatial frequency (cycles degree^{-1}), e is retinal eccentricity (degree), CT_0 is minimal contrast threshold, e_2 is half-resolution eccentricity constant, α spatial frequency decay constant and CT (f, e) is visible contrast threshold as a function of f and e.

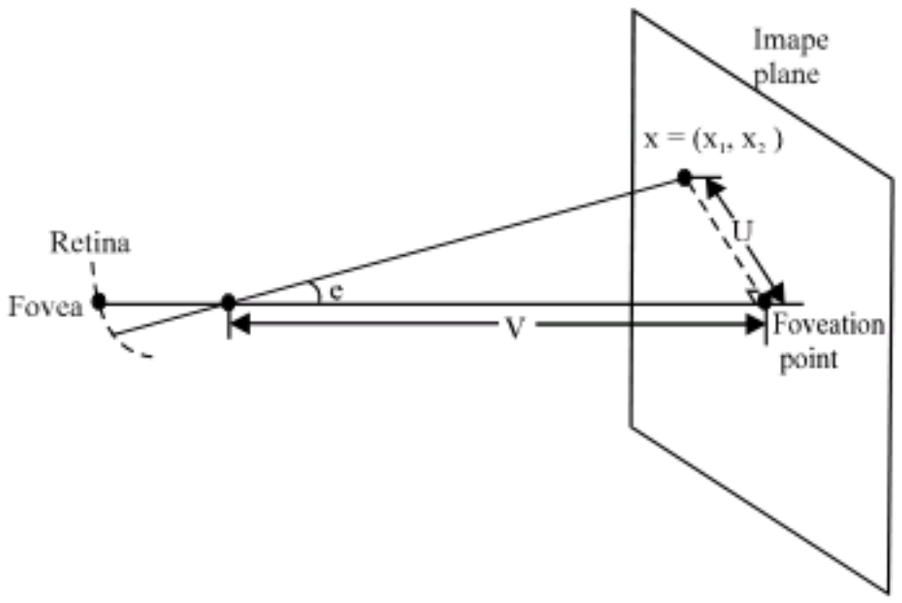

Fig. 3: Geometry relation between foveation point and given point

Generally, the best-fit parameter values for HVS are, α = 0.106, e = 2.3 degree and CT_0 1/64. For a given eccentricity e, Eq. 3 can be used to find its cut-off frequency f_c by setting CT = 1.0 (the maximum possible contrast). The result is further shown as:

$$f_c = \frac{e_2 \ln(1/CT_0)}{\alpha(e+e_2)} \tag{4}$$

Equation 4 indicates the computation relation between f_c and e for each pixel in the viewing image. In order to apply these models to digital images, we need to calculate the eccentricity e, for any given point or location in the image. A typical viewing geometry relation is shown in Fig. 3.

Obviously, the eccentricity e is calculated by:

$$e_c = 180 \cdot tg^{-1}(D \cdot l / V)/\pi \tag{5}$$

where, D is monitor dot itch (m), generally, $D = 0.25\times10^{-3}$; V, viewing distance (m); *l* is the distance between given point c and foveation point:

$$l = \left(x_c^2 + y_c^2\right)^{\wedge}(1/2)$$

On the other hand, in real-world digital images, the maximum perceived resolution f_m in the monitor is also limited by the display resolution f_m, which is shown as:

$$f_m = \pi/((tg^{-1}((D \cdot (l+1)/V - tg^{-1}((D \cdot (l-1)/V)\times180) \tag{6}$$

Equation 6 means that this distance is then used to determine the maximum spatial frequency (in cpd) which the monitor can reproduce at each pixel (maxfreq). Next, the maximum frequency of the monitor is divided by the maximum frequency resolvable by the visual system at each pixel:

$$Pyrlevel = f_m / f_c \tag{7}$$

This result, pyrlevel, corresponds to the (fractional) pyramid level which is required to be sent at each point in the image.

The pyrlevle matrix for one image may contain values less than 1. This occurs when the maximum spatial resolution resolvable by the eye is greater than the maximum resolution which the screen can display. Since, the display is a limiting factor, the pyrlevel matrix must be truncated at 1.0, which corresponds to the highest-resolution pyramid level. Conversely, the pyrlevel matrix may contain values which are larger than the computed highest pyramid level. In this case, pyrlevel is again truncated in order to stay within the bounds of the computed pyramid. This will produce a matrix containing foloating-point values between 1 and the number of pyramid levels which have been computed. In order to use this matrix, each pyramid level is blurred and upsampled in order to make each pyramid image the same size as the original. These images form a 3-D dataset. The value at each point in the foveated image is computed by linear interpolation between images in the 3-D dataset based on the floating-point pyramid value.

Finally, in order to apply foveation techniques to color images, we design that color fidelity is maintained by the use of the YCbCr transformation. When an RGB image is read in, it is converted to the YCbCr color space in order to separate luminance information from chrominance information. As long as each channel is treated identically, it should not make a great deal of difference which values are used during foveation. However, if it is desired that chrominance information be foveated to a greater degree than luminance information, then YCbCr color space would be the preferred choice.

Up to now, a foveated version of multi-resolution pyramid from an original uniform-resolution image is computed without the abrupt transitions between pyramid levels. In fairness, this technique should not be used in applications where computational speed is a priority. Since, a 3-D interpolation is required at each pixel, the required computation is nontrivial. However, in cases where remote transmission is a severely limiting factor, substantial processing time may be available for computation at the receiving processor as it waits for news data.

Space variant resolution imaging for image compressing: In order to apply the foveation framework described above to image compressing, we conceive a standard framework for transmitting the necessary data. Specifically, only those absolutely necessary portions of

the multi-resolution pyramid should be transmitted. Luckily, we have already computed the pyrlevel structure, which can be used to determine the pixels which are necessary for linear interpolation. A typical linear interpolation expression is shown by:

$$y = y_1 + \frac{y_2 - y_1}{x_2 - x_1}(x - x_1) \quad (8)$$

where, (x_1,y_1) and (x_2,y_2) are the coordinate of given points. In order for the receiver to be able to compute its own pyrlevel structure for reconstruction, the x and y coordinates of the foveation point must be transmitted, as well as the normal viewing distance and size of the original image. With only this small amount of information, the pyrlevel structure should be uniquely determined.

Next, the transmitter should send each level of the pyramid, taking care not to transmit unnecessary information. Therefore, pyrlevel is checked for each pixel in each pyramid level. If the pyrlevel value at the appropriate pixel location is large enough that the pixel in question will not be required for the linear interpolation, then, that pixel in the pyramid will not be transmitted. Since, the receiver also has a copy of the pyrlevel matrix, it can also determine which pixels should be sent. Therefore, the transmitter and receiver can remain in synchrony without extra bandwidth used for defining which pixels are to be sent.

In addition to the pyramid encoding, the image data should be compressed before transmission using some linear encoding mechanism such as Huffman coding. Using a linear code, the receiver can unpack the image data progressively as it is received, without having to wait for the entirety of the data to be received. This, in conjunction with encoding using a Laplacian pyramid, should produce substantially compressed images.

If the data is sent starting at the lowest-resolution level, then the receiving computer can progressively render the image as it is received. This will allow the used to monitor the progress of the downloaded, as well as allowing the user to see gross image attributes before all the data has been transmitted.

SOME IMPLEMENTATION RESULTS

Simulation of foveation with a fox image: In order to display space variant imaging simulating foveated images, we build the corresponding MATLAB programs with method described above and run them on a general-purpose computer (a Pentium D CPU 2.8 GHz under Windows XP).

Fig. 4: Original fox image with uniform resolution and the gaze point with blue arrow

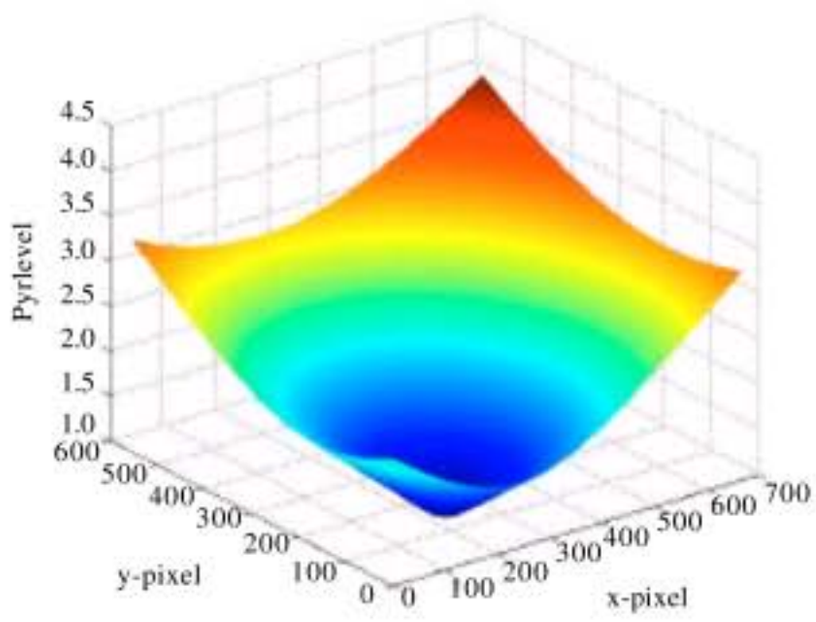

Fig. 5: Distribution of pyrlevel with each pixel

As an example, consider the large high-resolution fox image in Fig. 4. First, the blue arrow points to the region selected by the viewer. Second, the degree of foveation is calculated for each point within the image at a viewing distance of 1.0 m. The resulting pyrlevel matrix is shown three-dimensionally in Fig. 5. In the central fovea, this distribution is truncated due to the finite resolution of the monitor compared to the resolving capabilities of the eye. The maximum value of pyrlevel is just above Fig. 4, indicating that a six level pyramid is sufficient to foveate the full extent of the image. If fewer pyramid levels are desired, the maximum value of the pyrlevel structure must be limited to the number of pyramid levels actually computed. The resulting corresponding space-variant resolution is shown two dimensionally in Fig. 6, where, white means higher resolution and back means lower resolution, respectively. Obviously, the resolution has the highest value point of the fovea and drops rapidly away from that point as a function of eccentricity from the Fig. 1.

Fig. 6: Distribution of resolution with each pixel

Fig. 8: Step discontinuities of varying resolution

Fig. 7: Foveated version of uniform resolution Fig. 4

Fig. 9: Foveated image at viewing distance of 0.5 m

Next, this pyrlevel structure was used to generate a foveated image. Using linear interpolation described in Eq. 8 between pyramid levels, Fig. 7 was obtained. In this foveated image, there are no step discontinuities and the blurring appears to uniformly increase away from the foveation point. However, from the earlier study, the ring artifacts around each step boundary are quite noticeable. Even when fixating on the right gaze as calculated for the image, the ring artifacts are noticeable in the peripheral vision. An example using such an approach is shown in Fig. 8. The reason is that the most common approach to this is to use a floor operation to convert level numbers from the pyrlevel matrix into integers. Hence, in order to reduce this effect, interpolation between pyramid levels is necessary.

Another, we experiment on image resolution with different viewing distances in the same gaze point. Some implementation results based on Fig. 4 are shown in Fig. 9-11. As shown in Fig. 9-11 with the increase of viewing distance, the image at the same distance from the

Fig. 10: Foveated image at viewing distance of 1.5 m

Fig. 11: Foveated image at viewing distance of 2.0 m

Fig. 12: Foveated image with two points of gaze

Fig. 13: Foveated image in data compression by a factor of 3.9 at viewing distance of 3.0 m

gaze point become increasingly vague and the effective human visual range reduces accordingly. This multi-scale effect better complies with the real situation of human visual perception.

Finally, this presented technique is not limited to single-fovea images. Figure 12 shows an image which is foveated using two foci of gaze, where this is implemented by computing two separate pyrlevel matrices and at each pixel in the image, the lower of the two prylevel values is used.

Compression through space variant resolution of foveation: The motivation behind foveation image processing is that there exists considerable high-frequency information redundancy in the peripheral regions, thus a much more efficient representation of images can be obtained by removing or reducing such information redundancy. In other words, the human cannot distinguish between the original and the foveated versions of that image when their eyes gaze at the point of fixation. As for vision quality, there is undistorted information from foveated imaging for viewer. In this study, compression of image was achieved by saving the required data for the above reconstructions as a Laplacian pyramid. This foveation resulted in data compression by a factor of 5.9 is shown in Fig. 13.

In general, foveation produces significant storage savings over standard Laplacian pyramid compression. Foveation of image Laplacian pyramid encoding is further compressed. Table 1 shows the percent compression when compared to standard Laplacian pyramid encoding for ten images under some different points of gaze. Table 1 shows gains in compression were highly correlated with the size of the image to be encoded. For large high-resolution images, compression ratios exceeded 80%. For image sizes which are typical on web today, compression ranged from 20-30%. In these cases, the compression ratio was more strongly dependent on the exact placement of the point of gaze. Typically, from the experiment results shown in Table 1, where, resolution of

Table 1: Percent compression by foveation with image size in pixel and the eccentricity degree of foveation point away from center of image when compared to standard Laplacain pyramid encoding

	e (degree)					
	0	5	10	15	20	25
Size	(%)					
1.0s	18	20	21	23	25	29
1.6s	20	22	25	27	28	32
2.0s	21	24	27	28	31	33
2.2s	25	28	31	32	34	36
4.0s	29	40	42	44	46	47
5.2s	34	45	50	51	53	55
5.8s	37	49	52	54	59	62
6.2s	52	58	60	62	67	69
8.0s	60	72	78	78	79	72
9.0s	71	79	80	81	83	84

s: 10^5 pixel

the selected object images are given the first vertical line of Table 1, where s represents 1×10^5 pixels. For example, 1.0s means the resolution of the image is 1.0×10^5 pixels. Eccentricity (degrees) of the gaze points from the image center are given in the first horizontal line. Other data in Table 1 show the better image compression rates compared with the standard method under the same condition. As shown in Table 1, there are increasing compression rates away from center of foveated image, or higher eccentricity e. In this experiment, we find that the variation of compression results with gaze points is a complex question, which may result from the variation sensitivity of HSV with image content and gray value.

DISCUSSION

Simulating human visual system is a challenging study in computer vision. In this study, the presented method approaches closer to the biological fact of visual perception compared with traditional uniform image processing methods. As the significance of this study, this presented technique is a new image compressing technology inspired from HVS and may be applied to artificial retinal. This will be important in low bandwidth communication. Today, the Internet data communication is facing more and more challenges with increasingly large-sized image browsers. The use of foveation can be great benefits in reducing transmission time and bandwidth. These benefits can be realized without the aid of an eye-tracking device although the resultant blur will be noticeable to the observer. Especially, these biologically inspired methods of image compression and progressive image transmission have certain niche applications. Those widely and successfully applied image compression standards are not likely to change soon in order to accommodate these specialized situations. Hence, an efficient image processing method is more important in computer vision. Will the image processing method simulating retinal imaging be a new image compression standard? The answer may be yes and finding new biologically inspired methods of image compression for implementing special purposes may well be worthy of future working.

CONCLUSION

In this study, we describe the processing of space-variant resolution simulating foveated images. In order to approximate retinal imaging in the HVS, the Laplacian and Gaussian multi-resolution pyramids based on HVS weighing function is presented for space variant resolution techniques of foveation. From some implementation results above, this presented method resolve the ring artifacts around the step boundary between prylevels in the earlier study. Improved compressibility of foveation image is achieved by generating a Laplacian image pyramid. Further, the implementation results of compression rate related with the placement of the point of gaze are firstly shown in this study.

ACKNOWLEDGMENT

It is a study supported by National Basic Research Program of China (Program 973), No. 2007CB311005-01. And author would like to especially thank anonymity reviewers for their contribution.

REFERENCES

Bandera, C. and P. Scott, 1989. Foveal Machine Vision Systems. IEEE ICSMC, Cambridge, MA.

Camacho, P., F. Arrebola and F. Sandoval, 1996. Shifted Fovea Multiresolution Geometries. IEEE ICIP, New York.

Chang, E.C. and C. Yap, 1997. A wavelet approach to foveating images. Proceedings of the 13th ACM Symposium Computational Geometry, Jun. 4-6, France, pp: 397-399.

Chang, E.C., S. Mallat and C. Yap, 2000. Wavelet foveation. Applied Comput. Harmonic Anal., 9: 312-335.

Chang, C.C., Y.C. Lic and C.H. Lina, 2008. A novel method for progressive image transmission using blocked wavelets. Int. J. Elect. Commun., 62: 159-162.

Cormack, L.K., 2000. Computational Models of Early Human Vision. Handbook of Image and Video Processing Academic, New York.

Didenko, V., S. Lee, L.S. Roch and B. Silbermann, 2007. Approximate foveated images and reconstruction of their uniform pre-images. J. Approximation Theory, 147: 11-27.

Geisler, W.S. and J.S. Perry, 1998. A real-time foveated multiresolution system for low-bandwidth video communication. Proc. SPIE., 3299: 1-3.

Itti, L., 2004. Automatic foveation for video compression using a neurobiological model of visual attention. IEEE Trans. Image Process., 13: 1304-1308.

Kortum, P. and W.S. Geisler, 1996. Implementation of a foveated image coding system for image bandwidth reduction of video images. Proceedings of the SPIE: Human Vision and Electronic Imaging, Apr. 22, University of Texas Center for Vision and Image Sciences, pp: 350-360.

Kumwilaisak, W., 2008. Foveation image coding with fuzzy-based joint parameter selection. J. Visual Commun. Image Representation, 19: 450-463.

Kuyel, T., W. Geisler and J. Ghosh, 1999. Retinally reconstructed images: Digital images having a resolution match with the human eyes. IEEE Trans. Syst. Man Cybernet. Part A, 29: 235-243.

Lee, S., M.S. Pattichis and A.C. Bovik, 2001. Foveated video compression with optimal rate control. IEEE Trans. Image Process., 10: 977-992.

Lee, S., M.S. Pattichis and A.C. Bovik, 2002. Foveated video quality assessment. IEEE Trans. Multimedia, 4: 129-132.

Somma, G., 2006. Dynamic foveation model for video compression. Proceedings of the 18th International Conference on Pattern Recognition, Aug. 20-24, ICPR., pp: 339-342.

Thamcheewan, P., W. Kumwilaisak and P. Lasang, 2007. Foveated wavelet image coding with fuzzy logic. Proceedings of the Advanced Communication Technology, the 9th International Conference, Feb. 12-14, IEEE, pp: 1103-1108.

Tsumura, N., C. Endo, H. Haneishi and Y. Miyake, 1996. Image compression and decompression based on gazing area. Proceedings of the SPIE: Human Vision and Electronic Imaging, Jan. 29 - Feb. 1, Academic Press, pp: 361-367.

Wallace, R.S., P.W. Ong, B.B. Bederson and E.L. Schwartz, 1994. Space variant image processing. Int. J. Comput. Vision, 13: 71-90.

Wandell, B.A., 1995. Foundations of Vision. 1st Edn., Sinauer Associates, Inc., Sunderland, MA.

Wang, Z. and A.C. Bovik, 2000. Embedded foveation image coding. IEEE Trans. Image Process., 10: 1397-1410.

Wang, L.J., T. Horiuchi and H. Kotera, 2007. HDR image compression by local adaptation for scene and display using retinal model. IEICE Trans. Inform. Syst., E90: 173-181.